Hindawi
Complexity
Volume 2020, Article ID 6660117, 13 pages
https://doi.org/10.1155/2020/6660117

Research Article

A Cluster-Head Rotating Election Routing Protocol for Energy Consumption Optimization in Wireless Sensor Networks

Jun Wang[1], **Zhuangzhuang Du**[2], **Zhengkun He**[3] and **Xunyang Wang**[4,5]

[1]*School of Electrical Engineering, Henan University of Science and Technology, Luoyang, Henan 471000, China*
[2]*School of Agricultural Equipment Engineering, Henan University of Science and Technology, Luoyang, Henan 471003, China*
[3]*School of Computer Science and Engineering, Central South University, Changsha, Hunan 410000, China*
[4]*Department of Applied Mathematics, Lanzhou University of Technology, Lanzhou, Gansu 730050, China*
[5]*Postdoctoral Research Station in Gansu Electric Power Research Institute, Lanzhou, Gansu 730000, China*

Correspondence should be addressed to Xunyang Wang; 12198114@163.com

Received 31 October 2020; Revised 2 December 2020; Accepted 10 December 2020; Published 21 December 2020

Academic Editor: Yongsheng Hao

Balancing energy consumption using the clustering routing algorithms is one of the most practical solutions for prolonging the lifetime of resource-limited wireless sensor networks (WSNs). However, existing protocols cannot adequately minimize and balance the total network energy dissipation due to the additional tasks of data acquisition and transmission of cluster heads. In this paper, a cluster-head rotating election routing protocol is proposed to alleviate the problem. We discovered that the regular hierarchical clustering method and the scheme of cluster-head election area division had positive effects on reducing the energy consumption of cluster head election and intracluster communication. The election criterion composed of location and residual energy factor was proved to lower the probability of premature death of cluster heads. The chain multihop path of intercluster communication was performed to save the energy of data aggregation to the base station. The simulation results showed that the network lifetime can be efficiently extended by regulating the adjustment parameters of the protocol. Compared with LEACH, I-LEACH, EEUC, and DDEEC, the algorithm demonstrated significant performance advantages by using the number of active nodes and residual energy of nodes as the evaluation indicators. On the basis of these results, the proposed routing protocols can be utilized to increase the capability of WSNs against energy constraints.

1. Introduction

As the cornerstone of the system of the Internet of Things, wireless sensor networks (WSNs) are distributed network systems in which numerous microsensor nodes cooperate to detect, process, and transmit various information of interest in the way of wireless [1, 2]. Due to the characteristics of low cost, rapid deployment, self-organization, and high fault tolerance, WSNs have been widely used in numerous fields, such as military reconnaissance, environmental detection, agricultural production, and medical treatment [3–5]. Generally, the nodes powered by limited energy resource (batteries) are deployed in an unattended harsh environment, and it is virtually impracticable to replace or charge the depleted batteries after a long run [6, 7]. Therefore, in views of sustainability and quality of data acquisition, energy consumption reduction has become an essential issue for WSNs to lengthen the network lifetime.

Energy-efficient transmission and data aggregation mechanisms are critical subjects that cannot be ignored for energy saving in WSNs [8–10]. The primary aims to be achieved involve reducing the total energy consumption, decreasing the number of data communications, enhancing the number of active nodes over a certain period of operations, and balancing the energy dissipation of nodes [11–13]. Hierarchical cluster-based routing protocols have been considered as the most effective network organization scheme in improving the energy-efficiency for WSNs [14–16]. Recently, a variety of cluster routing algorithms of this type have been introduced to cope with the problems of

uneven load distribution among nodes and strict energy constraints [17, 18]. LEACH (low-energy adaptive cluster hierarchical) is the most classic clustering protocol [19]. However, with the increase of deployment scale, the efficiency of the protocol declines dramatically due to the single-hop communication from cluster heads (CHs) to the base station (BS) and the possibility of low-power nodes being repeated as CHs [20, 21]. Several dynamic CH role rotation algorithms have been suggested to eliminate the deficiencies of LEACH by multihops and energy awareness, including I-LEACH (improved low-energy adaptive cluster hierarchical) [22], EEUC (energy-efficient uneven clustering) [23], HEED (hybrid energy-efficient distribution) [24], DEEC (distributed energy-efficient clustering) [25], and DDEEC (developed distributed energy-efficient clustering) [26]. These block clustering-based protocols can alleviate unbalanced energy consumption through CH selection based on residual energy and more relevant criteria. Meanwhile, the mechanism of time-driven CH candidate is verified to be effective, easy to implement, and of low complexity [27, 28]. Nevertheless, the participation of each node in the CH election phase will unavoidably induce unnecessary energy loss, and it is remarkably challenging to obtain a satisfactory energy-efficiency of intracluster communication for the chosen CHs individually regarding their own location, energy level, or other related information [29–31]. Moreover, the irregular cluster distribution causes the intercluster communication path difficult to be optimal.

In addition, a series of chain clustering-based algorithms are exploited to increase the lifespan of the network along with sustainable scalability, such as PEGASIS (power-efficient gathering in sensor information systems) [32], CCM (chain cluster-based mixed) routing [33], and CCMAR (cluster-chain mobile agent routing) [34]. The use of chain-based routing protocols can significantly prolong network lifetime by minimizing transfer distance between nodes and avoiding the energy overhead of periodic head voting with a chain topology [35]. However, these algorithms suffer from colossal data delay and are not proper for large scale networks [36]. Through the above analysis, it can be inferred that the combination of advantages of both block clustering-based and chain clustering-based protocols is undoubtedly practicable and reliable option for energy-efficiency maximization in WSNs. Thus, we propose a cluster-head rotating election routing protocol (CHRERP) to efficiently manage energy consumption in this study. The main contributions of this study are summarized as follows:

(1) To reduce the number of nodes competing for CHs and the energy overhead in intracluster communication, the sensing area is segmented into multiple clusters by regular hierarchical pattern, and the central region in each cluster is utilized as the CH election area.

(2) The periodic time-based rotation of clusters and CH candidate areas is used to change cluster member composition and regulate node energy distribution dynamically.

(3) The node score evaluated by location and residual energy is adopted to select the CHs, and the chain shortest path with optimized intercluster communication dissipation is applied for data aggregation from clusters to the BS.

The remainder of this paper is arranged as follows. The network model and the energy consumption model are given in Section 2. The details of the presented routing algorithm are displayed in Section 3. The evaluations on the performances of the routing protocol and the impacts of key parameters are exhibited in Section 4. Finally, conclusions are shown in Section 5.

2. Preliminaries

2.1. Network Model. The network model used in this study is a WSN model in which N nodes are randomly deployed in a circular sensing area centered on a BS. The BS has strong computing and network management capabilities and is equipped with more battery power or can be self-replenished through energy harvesting. Hence, the BS can keep on working until all nodes are dead. On this basis, the following assumptions are made about the WSN.

(1) All nodes are homogeneous, stationary, and energy-constrained. The initial energy of each node is equal and expressed as E_0. Each node is assigned a unique identifier (ID) and can collect data packets from the cluster members when acting as a CH. CHs transmit data packets to the BS in single or multiple hops. In addition, the data packets are considered to be successfully transmitted upon arrival at the BS.

(2) The BS is aware of the location of every node after the network deployment. Each node stores the locations of other nodes and organization information in its database at the initial stage of the network through the BS's flooding broadcast.

(3) Proper medium access control methods (e.g., CDMA-based or contention window-based technologies) are applied to accomplish multiple simultaneous wireless transmissions.

2.2. Energy Consumption Model. According to the actual transmission distance from the CHs to the BS, the free space model and the multipath fading channel model both need to be comprehensively investigated; therefore, the extended model proposed in [37] is adopted in our study for representing communication energy consumption in consideration of path loss. Either the free space (d^2 power loss) or the multipath fading (d^4 power loss) channel models are included. The required energy for transmitting a m-bit packet is expressed as

$$E_T(m,d) = \begin{cases} E_{\text{elec}} \times m + m \times \varepsilon_{\text{fs}} d^2, & d < d_0, \\ E_{\text{elec}} \times m + m \times \varepsilon_{\text{mp}} d^4, & d \geq d_0, \end{cases} \quad (1)$$

where E_{elec} is the energy consumed per bit by the transmitter or receiver circuit, which depends on factors such as the

digital coding, modulation, filtering, and propagation of the radio signal. d is the distance between the transmitter and the receiver, and d_0 is utilized as the distance threshold. Moreover, in the case that $d < d_0$, we apply the free space model and ε_{fs} indicates the energy coefficient per bit. Otherwise, the multipath fading channel model is used, and ε_{mp} depicts the energy coefficient per bit.

The energy required to receive the data information of m bits is defined as follows:

$$E_R(m) = E_{elec} \times m. \tag{2}$$

3. Cluster-Head Rotating Election Routing Strategy

3.1. Cluster-Head Election Area. At the initialization stage of network, the BS evenly divides the sensing area into z sector districts and stratifies the sensing area with itself as the center according to different radiuses. The quantity of z directly reflects the density of clusters, and the greater the z value, the more clusters there are in the network. The region formed by the concentric rings of adjacent layers and the sector radius lines is regarded as a cluster area. Furthermore, within each sector district, a sector with a central angle of α is subdivided as the district's CH election area, and the part surrounded by the sector and each cluster area is further designated as the CH election area for the cluster. The position of CH election area is in the middle of the corresponding district (Figure 1).

For balancing energy consumption among nodes in a cluster, the CH rotating election method is adopted to decrease the possibility of an individual node being repeatedly selected as a CH. Specifically, all the districts and CH election areas rotate synchronically. Since each node can determine the cluster members after each rotation by the locations of the other nodes in the network and the rotation angle, non-extra-energy consumption of new cluster formation will generate. β is used to represent the counterclockwise rotation angle after the preset rounds of data collection (Figure 2).

Thus, the centerline angle of the n^{th} district, the center angle range of the n^{th} CH selection area, and the position of the n^{th} CH selection area after the p-round rotations can be computed by the following equations, respectively:

$$\theta_{Middle}(n) = \frac{2\pi n}{z} - \frac{\pi}{z}, \quad n \in (1, 2, 3, \ldots, z), \tag{3}$$

$$\theta_{Election}(n) = \left[\frac{2\pi n}{z} - \frac{\pi}{z} - \frac{\alpha}{2}, \frac{2\pi n}{z} - \frac{\pi}{z} + \frac{\alpha}{2}\right], \tag{4}$$

$$\theta_{Election}(p) = \left[\frac{2\pi n}{z} - \frac{\pi}{z} - \frac{\alpha}{2} + p\beta, \frac{2\pi n}{z} - \frac{\pi}{z} + \frac{\alpha}{2} + p\beta\right], \quad p \in z^{+}. \tag{5}$$

3.2. Hierarchical Pattern. Nodes close to the BS inevitably need to undertake more forwarding tasks. In this study, the competitive range of CH election of each layer is adjusted using the circular layered interval proportional to the distance from the BS (Figure 3), making up for the excessive energy consumption of CHs near to the BS. The hierarchical way can be expressed as follows:

$$\begin{cases} R_1 = r_0, & i = 1, \\ R_{i-0} = \varepsilon i r_0, & i \geq 2, \\ R_i = \varepsilon i r_0 - \varepsilon(i-1) r_0, & i \geq 2, \end{cases} \tag{6}$$

where R_1 denotes the radius of the first layer of the network, R_{i-0} represents the distance from the i^{th} layer to the BS, R_i depicts the width of the circular area of the i^{th} layer, R_0 implies the initial radius of the first layer, and ε $(0.5 \leq \varepsilon \leq 1.5)$ signifies the radius coefficient.

3.3. Cluster-Head Election Criterion. Following the network partitioned into clusters, it becomes a critical issue to select a suitable CH for each election area. Choosing the node near the centerline of the election area as the CH is beneficial to balance the transmission energy consumption within the cluster and reduce the communication distance between clusters. Nonetheless, considering only the location factor and ignoring the residual energy of the selected CHs, it is easy to cause premature failure for the low-energy CHs. In this study, the distance between the node and the corresponding centerline of the election area and the node residual energy are used as the candidate parameters for CH. The node score function for CH selection criteria can be depicted as follows:

$$CH_j = (1 - \chi)\frac{D_{max} - D_{jm}}{D_{max}} + \chi\frac{E_j}{E_0}, \tag{7}$$

where CH_j is the score of node j, χ $(0 \leq \chi \leq 1)$ is the weight adjustment coefficient, D_{max} is the half of the outer boundary length of the CH election area where node j is located, D_{jm} is the vertical distance from node j to the centerline of the election area, E_j is the residual energy of node j, and E_0 is the initial energy of node j. The node with the highest score for each election area is selected as the CH of the corresponding cluster.

3.4. Communication Process. After each rotation of districts and CH election areas, the nodes in each election area compute their scores associated with location and residual energy to decide whether they can become a CH. The chosen CHs in the same district then establish a chain communication link from outside to inside to deliver data packets collected from each cluster to the BS. The overall process of network communication is shown in Algorithm 1. Figure 4 illustrates the simulation result of the scenario ($N = 200$, $z = 4$, $i = 5$, and $\beta = 15^{\circ}$). As demonstrated in Figure 4(a), in the primary nonrotation phase, the selected CH of each

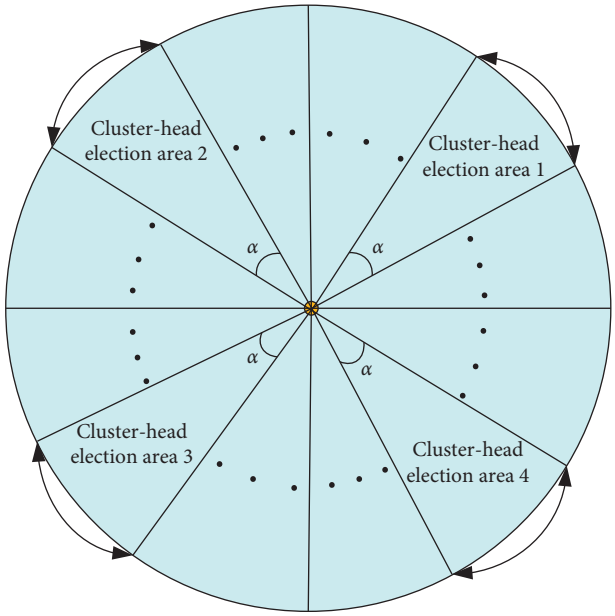

Figure 1: Initial distribution of CH election areas ($z = 4$).

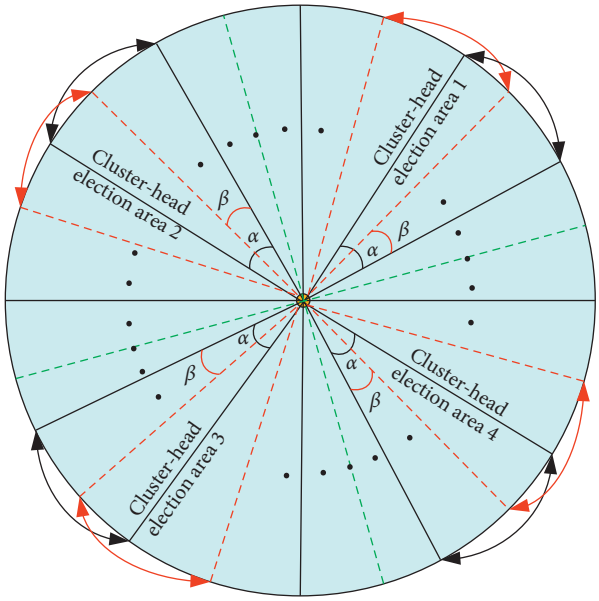

Figure 2: Rotation of CH election areas ($z = 4$, $\beta = 5^{\circ}$).

cluster is basically distributed near the centerline of the election area. After 45 rotations, the elected CHs obviously deviate from the centerlines with the change of node residual energy (Figure 4(b)).

4. Simulation Results and Analysis

To assess the performance of CHRERP in terms of network lifetime, relevant experiments are carried out with the help of MATLAB R2019a. The comparative tests with LEACH, I-LEACH, EEUC, and DDEEC are conducted under the same conditions, which are four cluster-based routing

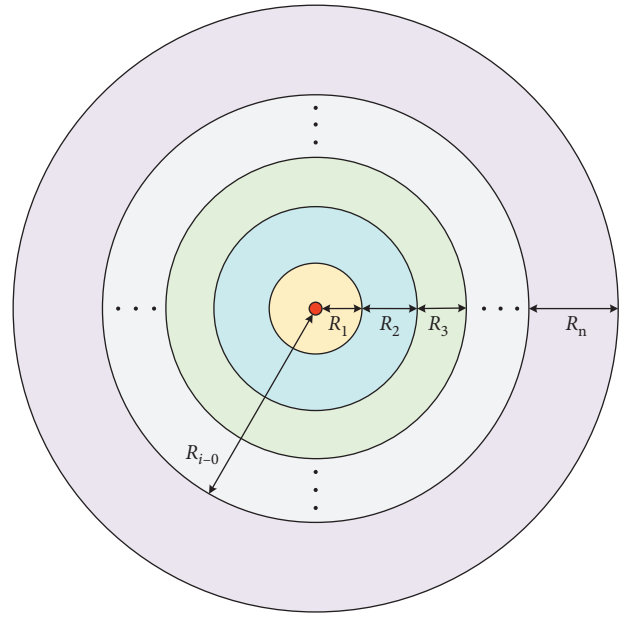

Figure 3: Heterogeneous multilayered network model.

protocols in WSNs. The values of the experimental parameters are shown in Table 1.

In the simulations, the influences of parameters ε, z, χ, α, and β on network lifetime are analyzed. The indexes, including the death round of the first node, the death round of half nodes, the death round of 80% nodes, and the residual energy after 80% node death, are used as assessment metrics.

Figure 5 depicts the assessment metrics with varying ε in the case of $z = 3$, $\chi = 0.9$, $\alpha = 30^{\circ}$, and $\beta = 5^{\circ}$. As manifested in Figure 5(a), with the increase of ε, the death round of the first node presents a decreasing trend, and the death round of both half and 80% nodes first increases and then decreases. When the death round of half and 80% nodes reaches the peak, ε is 1 and 2, respectively. The results show that, in the case that CH election areas do not rotate, the death round of the first node is inversely proportional to the deployment area of WSNs, which is consistent with most conventional algorithms. With the increase of simulation rounds, CHRERP can dramatically decrease the communication burden induced by the increase of the area, and an optimal interval of ε exists for a certain number of nodes. Moreover, the maximum of the weighted sum of death rounds is achieved when $\varepsilon = 2$, in the circumstance of the weight of the death round of the first node, half nodes, and 80% nodes is conventionally set to 0.1, 0.3, and 0.6, respectively. As exhibited in Figure 5(b), as ε goes from 0 to 4, the residual energy after 80% node death first increases and then decreases. The maximum residual energy is obtained in the case that ε is equal to 3, denoting that when ε is within the range [0, 3], the impact of ε on the residual energy is more significant than that of the growth of the sensing area. Nevertheless, as ε continuously grows, the energy consumption of nodes in the same cluster gradually increases with the rise of the sensing area, and the residual energy after 80% node death presents a downward trend. The size of the sensing area, interlayer distance, and clustering size can be

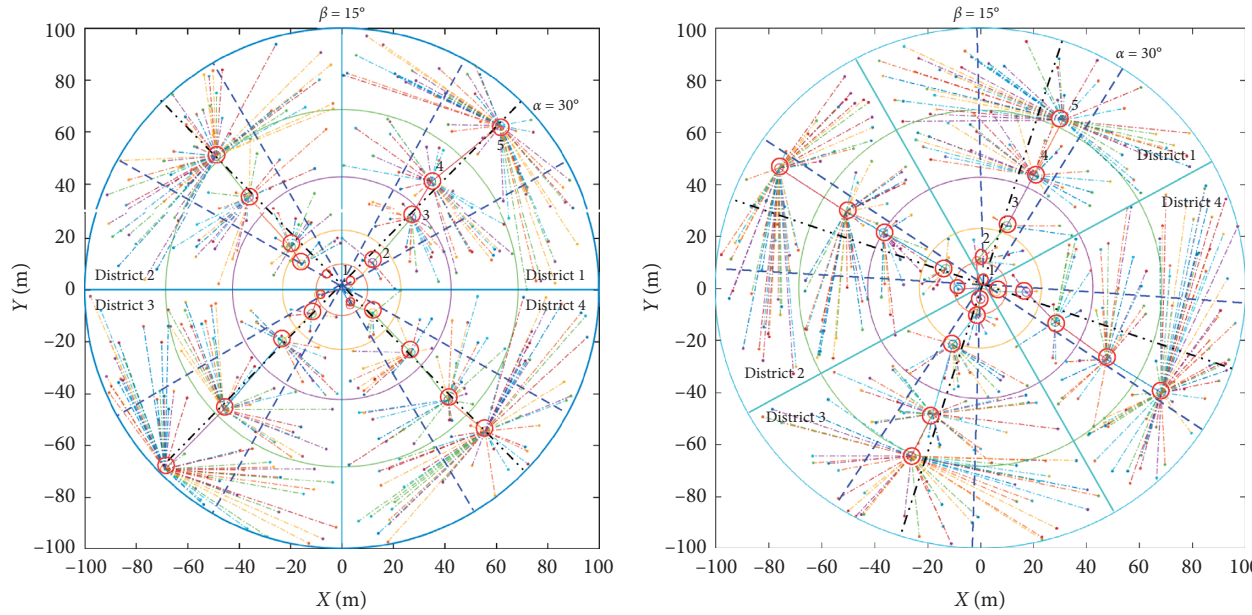

Figure 4: Illustration of network communication. (a) Nonrotation and (b) 45th rotation.

Input: Number of sector districts z, central angle of each CH election area α, weight adjustment coefficient χ, radius of the first layer r_0, number of layers i, radius coefficient ε, rotation angle β, location of each node, and number of data acquisition rounds per rotation, node morality threshold.
Output: Number of active nodes, residual energy.
Initialization: BS broadcasts the hierarchical clustering instruction. According to location, all the nodes are divided into a total of iz clusters numbered counterclockwise in ascending order.

(1) **While** Node death rate is below the set threshold **do**
(2) CH election, intra-cluster communication, inter-cluster communication.
(3) **for** $\beta \longleftarrow 0 < \theta \leq 2\pi/z$ **do**
(4) **repeat**
(5) **for** $j \longleftarrow$ Nodes in each CH election area **do**
(6) Calculate the score of nodes through equation (7);
(7) **end for**
(8) **until** Choose the node with the maximum score as the CH for each cluster; Execute pre-determined rounds of data acquisition; Rotate districts and CH election areas β degrees counterclockwise;
(9) **repeat**
(10) **for** Nodes within each cluster **do**
(11) Nodes transmit the data packets to the corresponding CH by single hop;
(12) **end for**
(13) **until** Each CH receives data packets from every active node in the cluster;
(14) **repeat**
(15) **for** CHs in the same district **do**
(16) CHs transfer data packets from outside to inside;
(17) **end for**
(18) **until** BS obtains data packets from the CHs in the first layer;
(19) **end for**
(20) **end**

Algorithm 1: Network communication procedure.

modified by regulating ε. It can be noticed that for the node number arranged in the simulation, ε between 1 and 2.5 has a positive effect on the number of simulation rounds, and ε varying from 2.0 to 3.0 can visibly enhance the residual energy. Furthermore, it can be inferred that an appropriate ε can adequately balance the node energy consumption of the whole network and extend the network lifetime. Hence, in the following simulation analysis, we choose ε as 2 hereafter

to determine the size of the sensing area and interlayer distance.

Figure 6 presents the assessment metrics with varying z under the case that $\varepsilon = 2$, $\chi = 0.9$, $\alpha = 30^{\circ}$, and $\beta = 5^{\circ}$. From Figure 6(a), It can be noted that with the rise of z, the number of death rounds declines noticeably. When $z = 5$, compared with the case of $z = 3$, the death round of the first node, half nodes, and 80% nodes reduces by 35.3%, 39.6%, and 57.5%, respectively. The growth of z will lead to the generation of more CHs. When the total number of nodes remains unchanged, the number of nodes in each cluster decreases relatively. As the number of simulation rounds rises, the probability of node being repeatedly selected as CH increases. Due to excessive energy consumption, the CHs will die prematurely while in the condition that z is small, the number of CHs in the network shrinks, and the number of nodes in each cluster increases, which can dramatically lower the chance of node becoming CH multiple times and boost the number of death rounds. It can be seen from Figure 6(b) that when z shifts from 3 to 8, the residual energy after 80% node death exhibits the characteristic of fluctuation, and when z is 3, the residual energy reaches the maximum. Therefore, for $z = 3$, the performance of assessment metrics is optimal, indicating that the CHRERP proposed in this paper are more suitable for the case with smaller z. Therefore, to optimize the network lifetime, we should reasonably adjust the network partition scale and avoid the premature death of partial nodes prompted by redundant CHs.

Figure 7 represents the effect of χ on the assessment metrics when $z = 3$, $\varepsilon = 2$, $\alpha = 30^{\circ}$, and $\beta = 5^{\circ}$. As shown in Figure 7(a), when χ changes between 0.3 and 0.7, the number of death rounds fluctuated slightly. While χ rises from 0.1 to 0.2 and 0.8 to 0.9, the death round of the first node, half nodes, and 80% nodes increases by −9, 918.4, 2087.6 and 22.2, 60.4, 419.4, respectively. Compared to $\chi = 0.9$, when $\chi = 0.2$, the number of the three death rounds grows by −73.8%, 30.6%, and 32.5%, respectively. It can be perceived that the case that χ equals 0.2 can adequately balance the weight relationship between node residual energy and the distance from node to the centerline of the candidate area and remarkably prolong the network lifetime. As presented in Figure 7(b), when χ is within the range of [0, 0.2], the residual energy after 80% node death is between 70 and 85 J. The residual energy declines drastically when χ varies from 0.3 to 1, proving that the smaller χ is more beneficial to improve the network energy-efficiency. It suggests that in the process of network operation, the effect of location factor on CH selection should be reinforced as much as possible.

Figure 8 expresses the impact of α on the assessment metrics in the circumstance that $\varepsilon = 2$, $z = 3$, $\chi = 0.9$, and $\beta = 5^{\circ}$. As seen in Figure 8(a), with the rise of α from 30° to 45°, the number of death rounds exhibits a downward trend as a whole. The death round of the first node, half nodes, and 80% nodes decreases by 1.9, 18.1, and 51.7 per degree, respectively. This decrease may be caused by the increase of energy consumption from the increment of participating nodes in the CH election and the path extension of intercluster communication. It can be seen from Figure 8(b) that when α increases from 30° to 45°, the residual energy after 80% node death remains between 35 and 40 J, inferring that α has little influence on the energy consumption of nodes. The simulation results show that a small α is in favor of balancing the network energy dissipation. In contrast, a larger α denotes the rise of each CH election area, definitely leading to the energy consumption increment of CH candidate process.

Table 1: Parameter values.

Parameter	Value
E_0	0.5 J
E_{elec}	50 nJ/bit
ε_{fs}	10 pJ/bit/m^2
ε_{mp}	0.0013 pJ/bit/m^4
d_0	87 m
r_0	30 m
I	5
Packet size	4000 bits
α	$30^{\circ} \le \alpha \le 45^{\circ}$
β	$5^{\circ} \le \beta \le 15^{\circ}$
z	$3 \le z \le 8$
ε	$0.5 \le \varepsilon \le 4$
χ	$0 \le \chi \le 1$
Number of nodes	1500
Number of data acquisition rounds per rotation	10

Figure 9 exhibits the relationships between β and the assessment metrics when $\varepsilon = 2$, $z = 3$, $\chi = 0.9$, and $\alpha = 30^{\circ}$. As observed in Figure 9(a), the variations of the three death rounds present notable differences. The death round of the first node performs an overall downward trend, and the number of death rounds reduces by 3.2 for per degree increment. The fluctuation of the death round of half nodes is stable, and the value changes around 1300 rounds. The death round of 80% nodes lowers sharply under the condition that β grows from 13° to 15°. The results indicate that a continuous increase in β will ultimately cause a drastic reduction in the number of simulation rounds. It can be recognized from Figure 9(b) that, in the case that β is within the range of 5° to 13°, the residual energy after 80% node death maintains between 35 and 40 J, while β jumps to 15°, and the residual energy falls below 35 J. To sum up, $\beta = 5^{\circ}$ can lengthen the network lifetime compared with a larger β. It may be caused by the fact that with the enlargement of β, the intersection of candidate areas decreases before and after each rotation, then the selected CH will unavoidably deviate from the centerline region due to the inconspicuous residual-energy advantage of nodes near the centerline for the updated election area.

Figure 10 displays the combination effect of χ and α on assessment metrics in the condition that $\varepsilon = 2$, $z = 3$, and $\beta = 5^{\circ}$. From Figure 10(a), when χ and α grow from 0.1 to 0.7 and from 30° to 45°, respectively, the fluctuation scale of each death round of the first node is little and has approximate waveform characteristics. When χ constantly rises from 0.7 and α is in the range of 30° to 45°, the death round enhances visibly, and [0.9, 30°] is the optimal combination of χ and α.

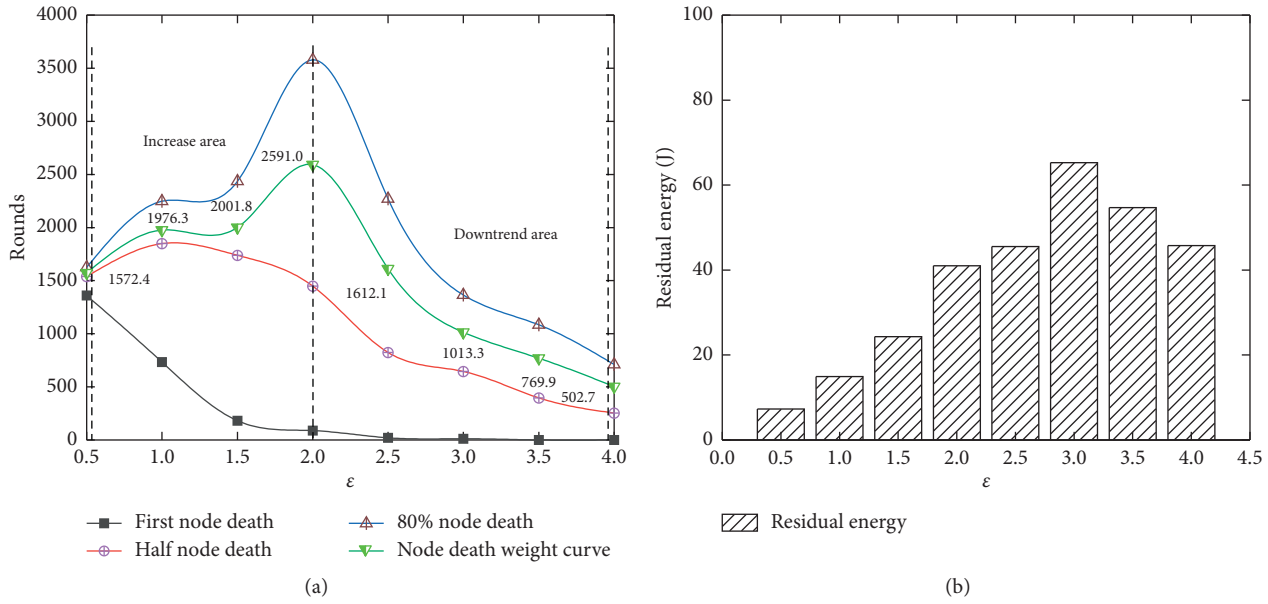

Figure 5: Assessment metrics with varying ε: (a) death round with varying ε and (b) residual energy with varying ε.

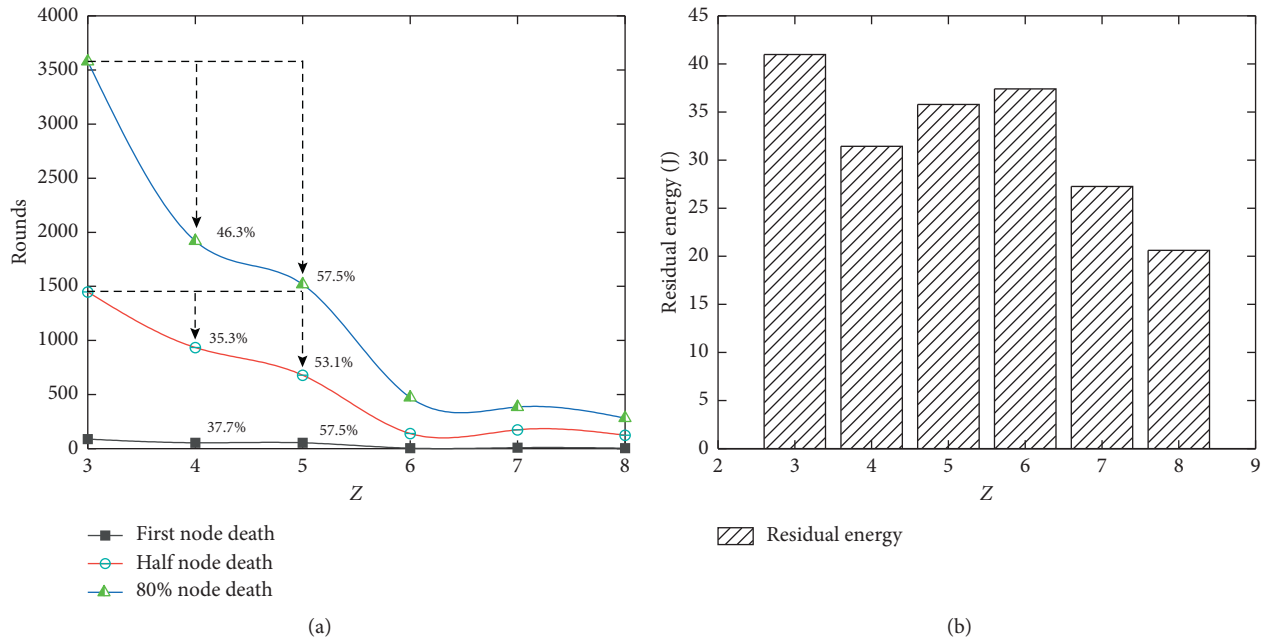

Figure 6: Relationships between z and assessment metrics: (a) influence of z on death round and (b) influence of z on residual energy.

In Figure 10(b), while χ changes from 0.3 to 0.7 and α rises from 30° to 45°, the death round of half nodes varies slightly. When χ increases from 0.7 to 0.9, the death round begins to ascend. However, compared with $\chi = 0.2$, the number of death rounds drops greatly, and the combination of [0.2, 30°] manifests the best performance. The identical fluctuation characteristics with Figure 10(b) can be discovered in Figure 10(c), and [0.2, 30°] is also the combination with the most extended network lifetime. As presented in Figure 10(d), when χ belongs to the range of [0.2, 0.9], the residual energy after 80% node death overall decreases and the most excellent performance is achieved at [0.2, 30°]. Obviously, the larger χ can increase the death round of the first node, while the smaller χ will unavoidably improve the death round of half nodes and 80% nodes. It can be easily concluded that the combination of χ and α with small values is more valuable for the extension of network lifetime.

Figure 11 manifests the combination influence of χ and β for assessment metrics when $\varepsilon = 2$, $z = 3$, and $\alpha = 30°$. It can be seen from Figure 11(a) that the death round of the first node declines by about 2.5 rounds on average per degree increment in β. When χ grades from 0.1 to 0.7, the death

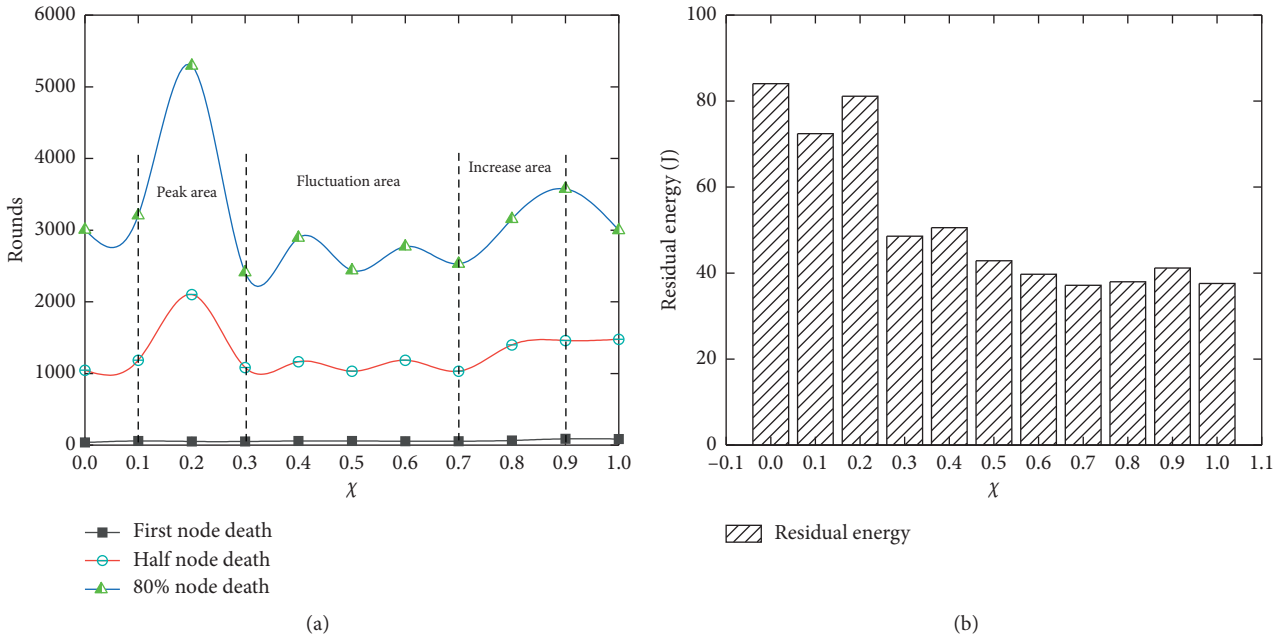

Figure 7: Assessment metrics with varying χ: (a) impact of χ on death round and (b) impact of χ on residual energy.

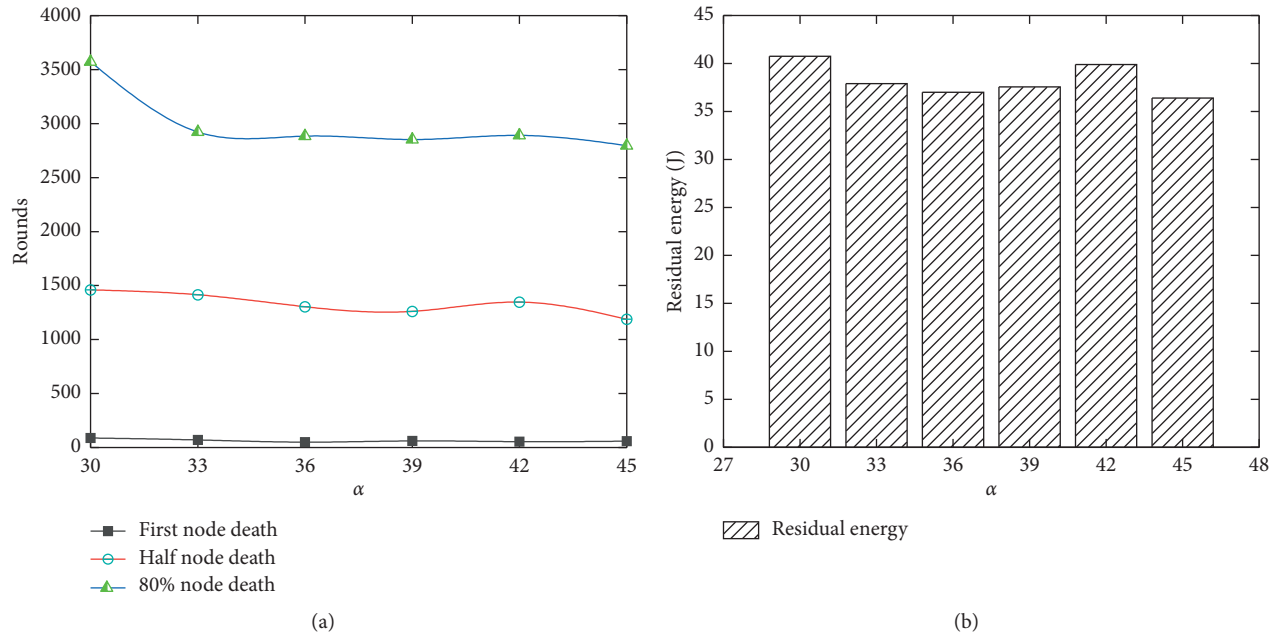

Figure 8: Affecting relations between α and assessment metrics: (a) death round with varying α and (b) residual energy with varying α.

round is stable. In addition, χ increases from 0.7 to 0.9, the number of death rounds for different β increases by 58.8%, 62.5%, 60.7%, 75.2%, 79.6%, and 103.3%, respectively, the combination parameter of [0.9, 5°] is the most proper selection. Figures 11(b) and 11(c) exhibited a similar variation pattern. When $\chi = 0.2$, the death round reaches the maximum. Only slight fluctuations in death round occur under the situation that χ is within the range of [0.3, 0.7]. Furthermore, the number of death rounds boosts with the increase of χ from 0.7 to 0.9, and the optimal combination is obtained at [0.2, 5°]. From Figure 11(d), it can be noticed that the residual energy after 80% node death gains the maximum when $\chi = 0.2$ and $\beta = 5°$. It can be inferred that the [0.2, 5°] can effectively mitigate the unbalanced energy consumption of nodes. Further, we can summarize that the optimized combination of χ and β has a profound impact on improving the number of death rounds and node residual energy.

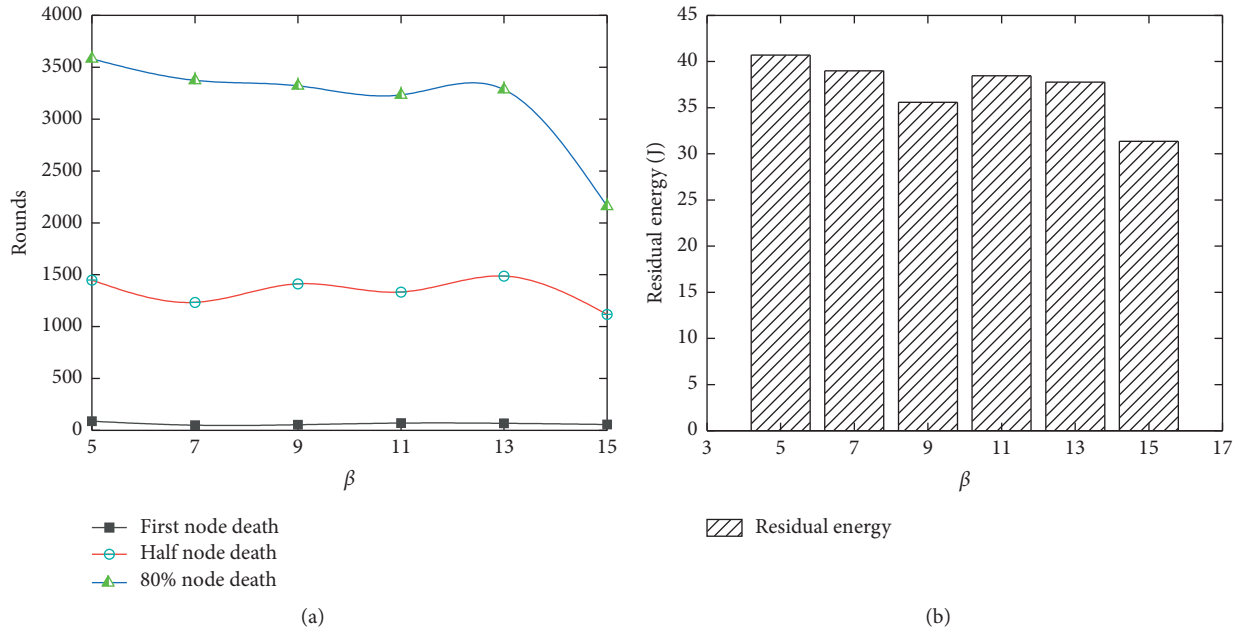

Figure 9: Relevance evaluation between β and assessment metrics: (a) effect of β on death round and (b) effect of β on residual energy.

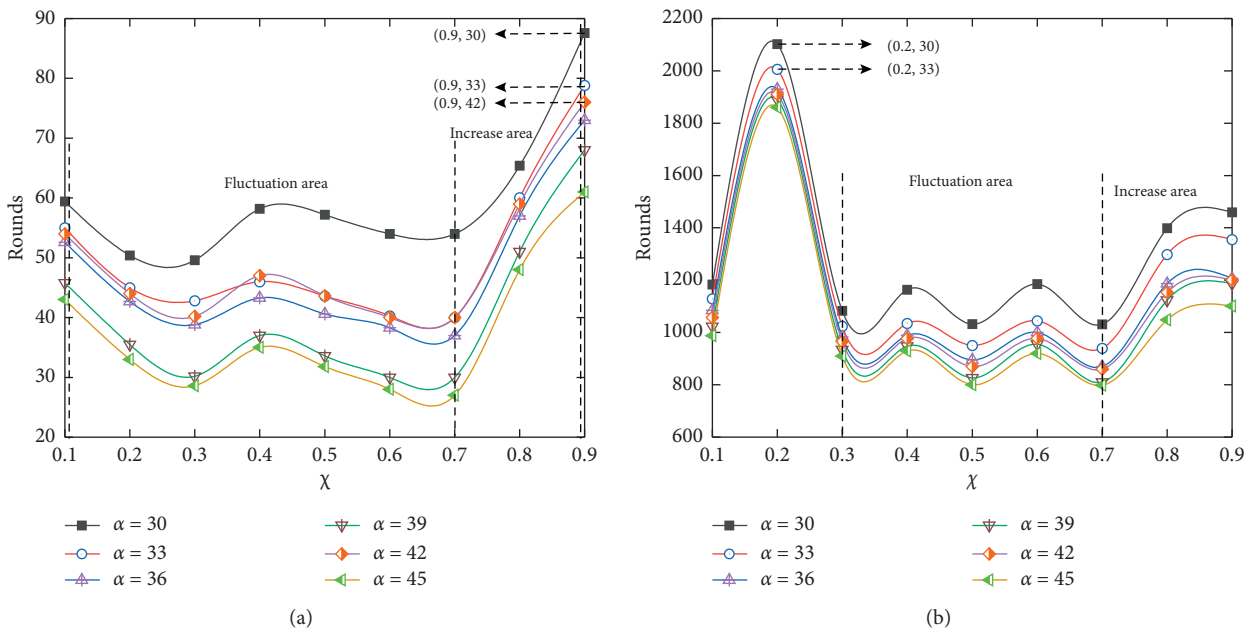

Figure 10: Continued.

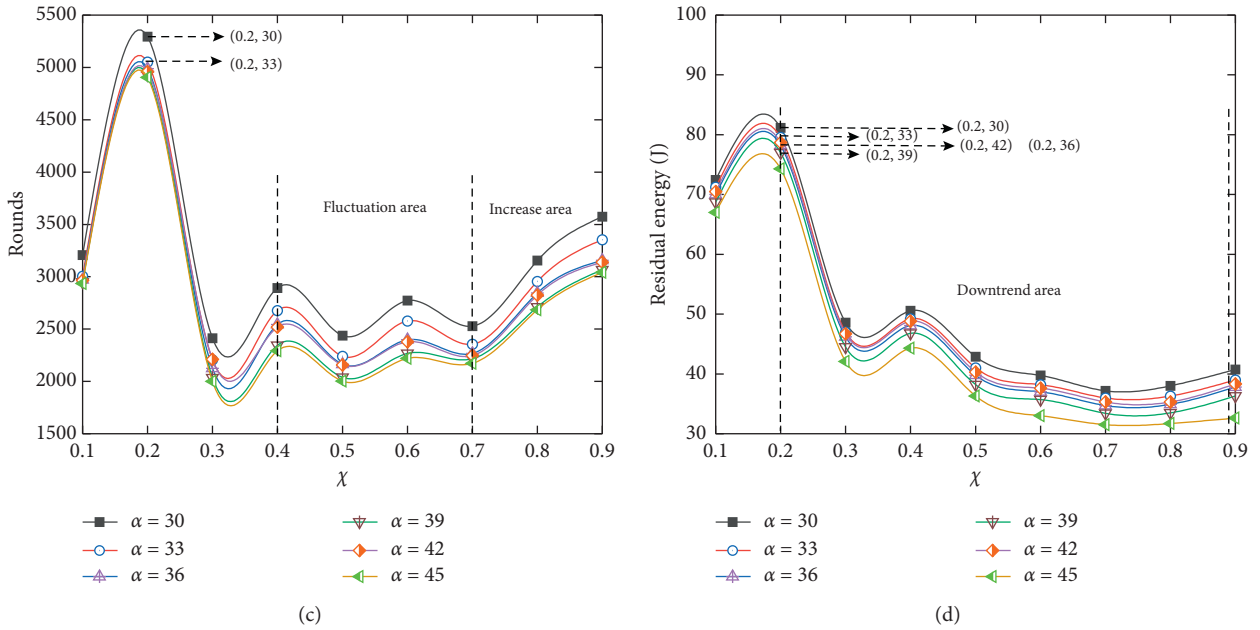

FIGURE 10: Combination impact of χ and α on assessment metrics, (a) death round of the first node with varying χ and α: (b) death round of half nodes with varying χ and α, (c) death round of 80% nodes with varying χ and α, and (d) residual energy with varying χ and α.

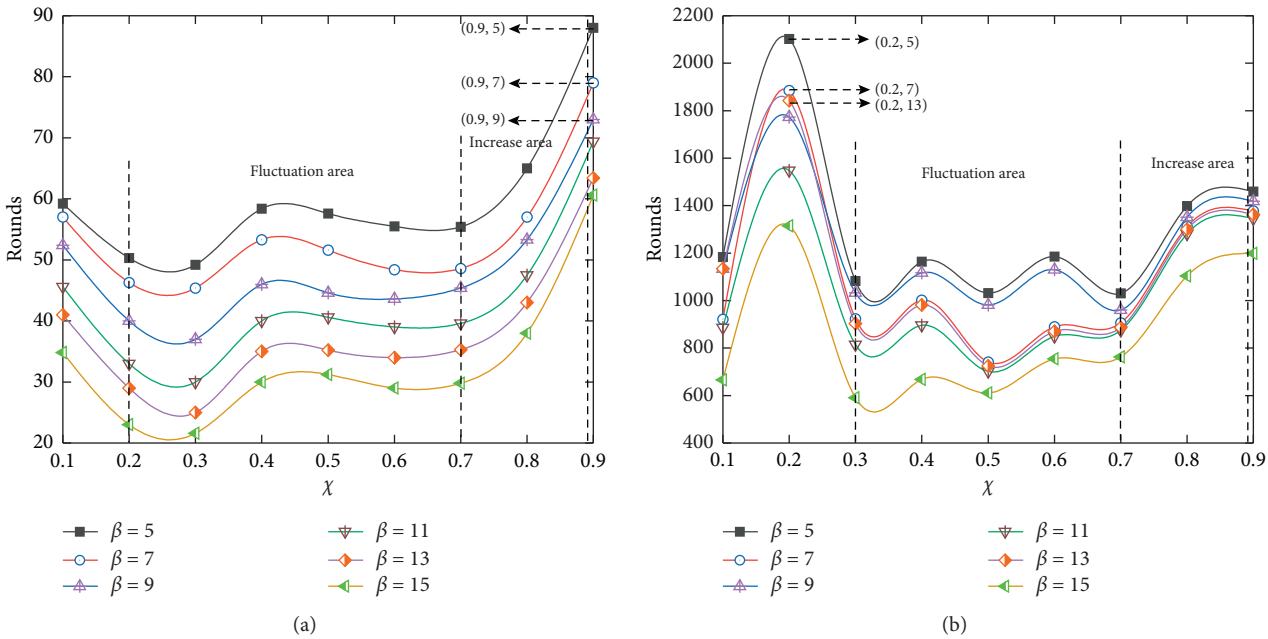

FIGURE 11: Continued.

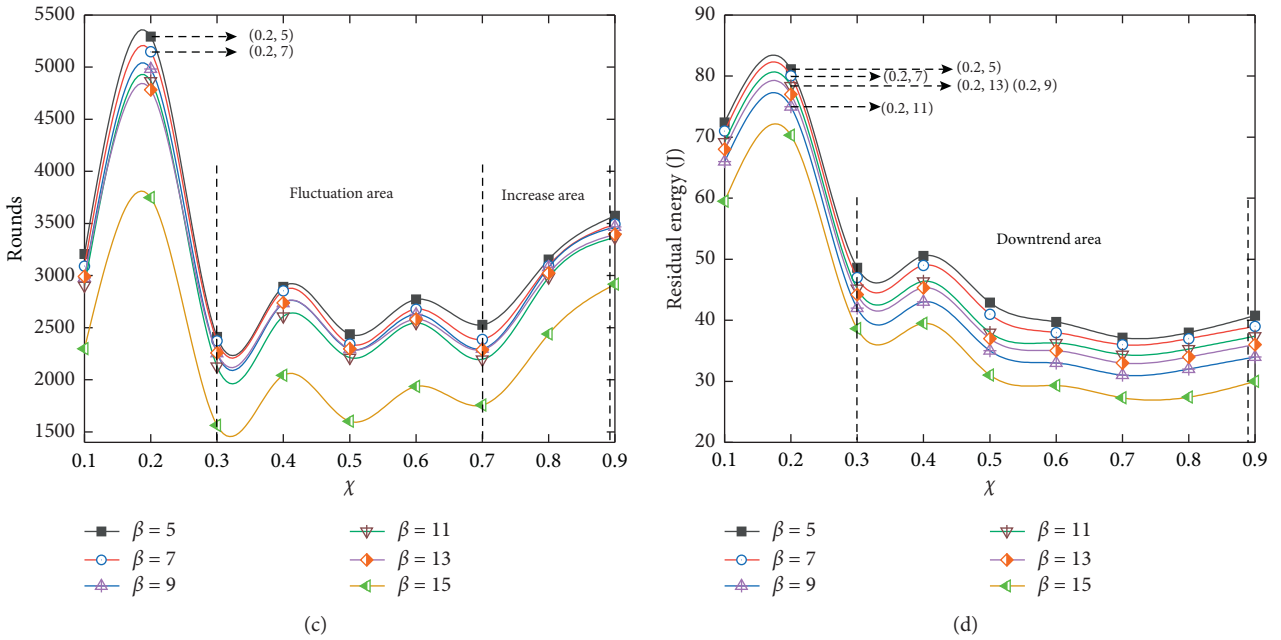

FIGURE 11: Relationships between $[\chi, \beta]$ and assessment metrics: (a) impact of $[\chi, \beta]$ on the death round of the first node, (b) impact of $[\chi, \beta]$ on the death round of half nodes, (c) impact of $[\chi, \beta]$ on the death round of 80% nodes, and (d) impact of $[\chi, \beta]$ on residual energy.

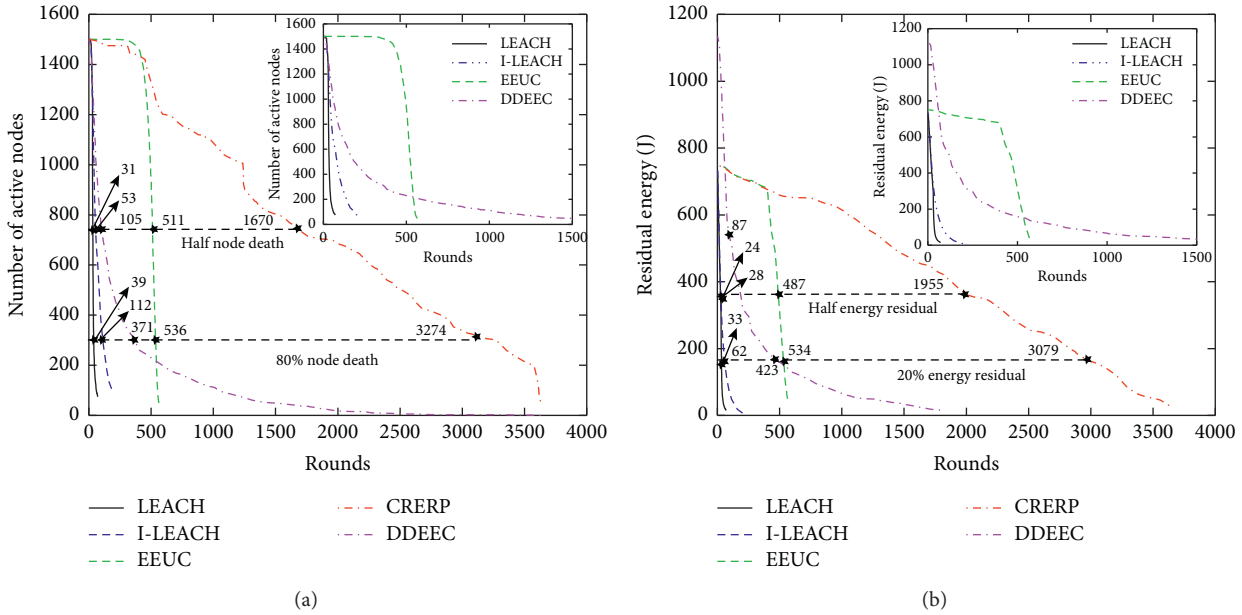

FIGURE 12: Performance comparisons of CHRERP, LEACH, I-LEACH, EEUC, and DDEEC: (a) number of active nodes with varying simulation rounds and (b) residual energy with varying simulation rounds.

Figure 12 shows the comparison results of CHRERP proposed in this study with LEACH, I-LEACH, EEUC, and DDEEC, by using the number of active nodes and residual energy of nodes as the evaluation indicators. As shown in Figure 12(a), in the case that the number of simulation rounds is less than 400, the number of active nodes of EEUC and CHRERP decreases mildly and keeps above 1400 nodes. However, when the number of simulation rounds continues to increase higher than 400 rounds, the number of active nodes of EEUC declines precipitously, and CHRERP presents a slow decline. Meanwhile, the death round of half nodes for LEACH, I-Leach, EEUC, DDEEC, and CHRERP is 31, 53, 511, 105, and 1670, and the death round of 80% nodes is 39, 112, 536, 371, and 3274, respectively. Compared with the other four protocols, CHRERP can hugely increase the number of active

nodes for the same simulation rounds. It is easily recognized that CHRERP can optimize the clustering specification of the network sensing area and rotate to elect CHs considering the location and residual energy, resulting in reducing the possibility of node being repeatedly selected as the CH and the intracluster communication distance. In addition, the "radial path" with the minimum number of hops is adopted for data transmission between clusters. All the factors mentioned above may contribute to the excellent performance of CHRERP. It can be seen from Figure 12(b) that the number of simulation rounds of LEACH, I-LEACH, EEUC, DDEEC, and CHRERP with half residual energy is 24, 28, 487, 87, and 1955, and the number of simulation rounds with 20% residual energy is 33, 62, 534, 423, and 3079, respectively. Moreover, the initial energy difference originates from the fact that LEACH, I-Leach, EEUC, and CHRERP are all for homogeneous WSNs, while DDEEC is used in heterogeneous WSNs comprising normal nodes and advanced nodes with higher energy. We can conclude that CHRERP has notable advantages in energy saving, due to selecting nodes with higher energy as CHs and establishing the shortest communication path between clusters.

5. Conclusions

In this study, based on the CH rotating election scheme, a novel hierarchical clustering routing protocol was proposed for WSNs to improve the network lifetime. The weighted ratio sum of location and residual energy information of nodes in each CH candidate area was used as the election criterion. We validated the performance of the developed protocol by applying the death round of the first node, the death round of half nodes, the death round of 80% nodes, and the residual energy after 80% node death as assessment metrics. The results indicated that a moderate radius coefficient was confirmed for the balancing effect on both operation rounds and total residual energy. Meanwhile, a fit number of sector districts could effectively prolong the network lifetime by regulating the number of CHs. Little χ, α, and β should be advised for reducing the network energy consumption. In addition, the influence of combined parameters [χ, α] and [χ, β] on the energy-efficiency of the network was consistent with that of an individual parameter. Compared with LEACH, I-LEACH, EEUC, and DDEEC, the addressed protocol exhibited an overwhelming advantage in terms of the number of active nodes and residual energy. Our simulation results suggest that CHRERP is a feasible method for mitigating the unbalanced energy consumption for intracluster and intercluster communication in WSNs. In future work, we will investigate the application of this protocol in a real-world wireless communication scenario to enhance the reliability and practicality of the protocol.

Data Availability

The data used to support the findings of this study are available from the corresponding author upon request.

Conflicts of Interest

The authors declare that there are no conflicts of interest regarding the publication of this article.

Authors' Contributions

J.W. conceptualized the study; J.W. and Z.D. developed methodology; Z.H. provided software; Z.D. and X.W. performed validation; J.W. performed formal analysis; J.W. and Z.D. performed investigation; J.W. provided resources; Z.D. and Z.H. performed data curation; J.W., Z.D., and X.W. prepared the original draft; Z.D. and X.W. reviewed and edited the article; Z.D. performed visualization; X.W. supervised the study; J.W. performed project administration; and J.W. was responsible for funding acquisition. All authors have read and agreed to the published version of the manuscript.

Acknowledgments

This research was funded by National Natural Science Foundation of China (Grant no. 61771184), Program for Science & Technology Innovation Talents in Universities of Henan Province (Grant no. 20HASTIT029), Program for Innovative Research Team (in Science and Technology) in University of Henan Province (Grant no. 19IRTSTHN021), and Science and Technology Major Project of Henan Province (Grant no. 181100110100).

References

[1] W. Wen, S. Zhao, C. Shang, and C.-Y. Chang, "EAPC: energy-aware path construction for data collection using mobile sink in wireless sensor networks," *IEEE Sensors Journal*, vol. 18, no. 2, pp. 890–901, 2018.

[2] J. Huang, Y. Hong, Z. Zhao, and Y. Yuan, "An energy-efficient multi-hop routing protocol based on grid clustering for wireless sensor networks," *Cluster Computing*, vol. 20, no. 3, pp. 3071–3083, 2017.

[3] Z. Zhao, K. Xu, G. Hui, and L. Hu, "An energy-efficient clustering routing protocol for wireless sensor networks based on AGNES with balanced energy consumption optimization," *Sensors*, vol. 18, no. 11, Article ID 3938, 2018.

[4] Y. Du, J. Gong, Z. Wang, and N. Xu, "A distributed energy-balanced topology control algorithm based on a noncooperative game for wireless sensor networks," *Sensors*, vol. 18, no. 12, Article ID 4454, 2018.

[5] D. Agrawal and S. Pandey, "FUCA: fuzzy-based unequal clustering algorithm to prolong the lifetime of wireless sensor networks," *International Journal of Communication Systems*, vol. 31, no. 4, Article ID e3448, 2018.

[6] R. Logambigai, S. Ganapathy, and A. Kannan, "Energy-efficient grid-based routing algorithm using intelligent fuzzy rules for wireless sensor networks," *Computers & Electrical Engineering*, vol. 68, pp. 62–75, 2018.

[7] L. Li and D. Li, "An energy-balanced routing protocol for a wireless sensor network," *Journal of Sensors*, vol. 2018, Article ID 8505616, 12 pages, 2018.

[8] B. S. Mostafa and B. A. Massoud, "HEEC: a hybrid unequal energy efficient clustering for wireless sensor networks," *Wireless Networks*, vol. 25, no. 8, pp. 4751–4772, 2018.

[9] H. Rhim, K. Tamine, R. Abassi, S. Damien, and G. Sihem, "A multi-hop graph-based approach for an energy-efficient routing protocol in wireless sensor networks," *Human-centric Computing and Information Sciences*, vol. 8, Article ID 30, 2018.

[10] M. Abbasi and N. Fisal, "Noncooperative game-based energy welfare topology control for wireless sensor networks," *IEEE Sensors Journal*, vol. 15, no. 4, pp. 2344–2355, 2015.

[11] Y. Zhang, M. Liu, and Q. Liu, "An energy-balanced clustering protocol based on an improved CFSFDP algorithm for wireless sensor networks," *Sensors*, vol. 18, no. 3, Article ID 881, 2018.

[12] G. Han and L. Zhang, "WPO-EECRP: energy-efficient clustering routing protocol based on weighting and parameter optimization in WSN," *Wireless Personal Communications*, vol. 98, no. 1, pp. 1171–1205, 2017.

[13] K. Guravaiah and R. Leela Velusamy, "Energy efficient clustering algorithm using RFD based multi-hop communication in wireless sensor networks," *Wireless Personal Communications*, vol. 95, no. 4, pp. 3557–3584, 2017.

[14] A. Emad and M. Ion, "New energy efficient multi-hop routing techniques for wireless sensor networks: static and dynamic techniques," *Sensors*, vol. 18, no. 6, pp. 3557–3584, 2018.

[15] B. Na, G. Han, L. Li, J. Xu, and S. Lei, "An unequal clustering routing protocol for energy-heterogeneous wireless sensor networks," in *Proceedings of the 2015 IEEE/CIC International Conference on Communications in China—Workshops (CIC/ICCC)*, Shenzhen, China, June 2017.

[16] K. Wang, Y. Ou, H. Ji, H. Zhang, and X. Li, "Energy aware hierarchical cluster-based routing protocol for WSNs," *The Journal of China Universities of Posts and Telecommunications*, vol. 23, no. 4, pp. 46–52, 2016.

[17] D. C. Hoang, P. Yadav, R. Kumar, and S. K. Panda, "Real-time implementation of a harmony search algorithm-based clustering protocol for energy-efficient wireless sensor networks," *IEEE Transactions on Industrial Informatics*, vol. 10, no. 1, pp. 774–783, 2013.

[18] A. Mehmood, Z. Lv, J. Lloret, and M. M. Umar, "ELDC: an artificial neural network based energy-efficient and robust routing scheme for pollution monitoring in WSNs," *IEEE Transactions on Emerging Topics in Computing*, vol. 8, no. 1, pp. 106–114, 2017.

[19] W. R. Heinzelman, A. Chandrakasan, and H. Balakrishnan, "Energy-efficient communication protocol for wireless microsensor networks," in *Proceedings of the 33rd Hawaii International Conference on System Sciences*, pp. 1–10, NW Washington, DC, USA, January 2000.

[20] D. Izadi, J. Abawajy, and S. Ghanavati, "An alternative clustering scheme in WSN," *IEEE Sensors Journal*, vol. 15, no. 7, pp. 4148–4155, 2015.

[21] V. Pal, G. Singh, and R. P. Yadav, "Balanced cluster size solution to extend lifetime of wireless sensor networks," *IEEE Internet of Things Journal*, vol. 2, no. 5, pp. 399–401, 2015.

[22] Z. Beiranvand, A. Patooghy, and M. Fazeli, "I-LEACH: an efficient routing algorithm to improve performance & to reduce energy consumption in wireless sensor networks," in *Proceedings of the 5th Conference on Information and Knowledge Technology*, pp. 13–18, Shiraz, Iran, May 2013.

[23] Z. Shen, F. Liu, B. Hou, and C. Zhang, "Energy-efficient uneven clustering routing protocol for wireless sensor networks," *Transducer and Microsystem Technologies*, vol. 32, no. 12, pp. 60–67, 2013.

[24] O. Younis and S. Fahmy, "HEED: a hybrid, energy-efficient, distributed clustering approach for ad hoc sensor networks," *IEEE Transactions on Mobile Computing*, vol. 3, no. 4, pp. 366–379, 2004.

[25] N. Javaid, T. N. Qureshi, A. H. Khan et al., "EDDEEC: enhanced developed distributed energy-efficient clustering for heterogeneous wireless sensor networks," *Procedia Computer Science*, vol. 19, pp. 914–919, 2013.

[26] A. Rathee, I. Kashyap, and K. Choudhary, "Developed distributed energy-efficient clustering (DDEEC) algorithm based on fuzzy logic approach for optimizing energy management in heterogeneous WSNs," *International Journal of Computer Applications*, vol. 115, no. 17, pp. 14–19, 2015.

[27] W. Mardini, M. B. Yassein, Y. Khamayseh, and B. A. Ghaleb, "Rotated hybrid, energy-efficient and distributed (R-HEED) clustering protocol in WSN," *WSEAS Transactions on Communications*, vol. 10, no. 20, pp. 16416–16420, 2015.

[28] G. Ma and Z. Tao, "A hybrid energy- and time-driven cluster head rotation strategy for distributed wireless sensor networks," *International Journal of Distributed Sensor Networks*, vol. 2013, no. 6, pp. 89–108, 2013.

[29] H. W. Ferng and J. S. Chuang, "Area-partitioned clustering and cluster head rotation for wireless sensor networks," in *Proceedings of the 2017 International Conference on Machine Learning and Cybernetics (ICMLC)*, Ningbo, China, July 2017.

[30] D. Lin, Q. Wang, D. Lin, and Y. Deng, "An energy-efficient clustering routing protocol based on evolutionary game theory in wireless sensor networks," *International Journal of Distributed Sensor Networks*, vol. 2015, pp. 1–12, 2015.

[31] O. A. Amodu and R. A. Raja Mahmood, "Impact of the energy-based and location-based LEACH secondary cluster aggregation on WSN lifetime," *Wireless Networks*, vol. 24, no. 5, pp. 1403–1408, 2013.

[32] S. Lindsey, "PEGASIS: power-efficient gathering in sensor information systems," in *Proceedings of the IEEE Aerospace Conference Proceedings*, pp. 1125–1130, Big Sky, MT, USA, February 2002.

[33] H. K. Farhan, "Enhanced chain-cluster based mixed routing algorithm for wireless sensor networks," *University of Baghdad Engineering Journal*, vol. 22, no. 1, pp. 103–117, 2016.

[34] S. Sasirekha and S. Swamynathan, "Cluster-chain mobile agent routing algorithm for efficient data aggregation in wireless sensor network," *Journal of Communications and Networks*, vol. 19, no. 4, pp. 392–401, 2017.

[35] F. Tang, I. You, S. Guo, M. Guo, and Y. Ma, "A chain-cluster based routing algorithm for wireless sensor networks," *Journal of Intelligent Manufacturing*, vol. 23, no. 4, pp. 1305–1313, 2012.

[36] S. Rani, S. H. Ahmed, J. Malhotra, and R. Talwar, "Energy efficient chain based routing protocol for underwater wireless sensor networks," *Journal of Network and Computer Applications*, vol. 92, pp. 42–50, 2017.

[37] W. B. Heinzelman, A. P. Chandrakasan, and H. Balakrishnan, "An application-specific protocol architecture for wireless microsensor networks," *IEEE Transactions on Wireless Communications*, vol. 1, no. 4, pp. 660–670, 2002.